



# Highly active Fenton-like catalyst derived from solid waste-iron ore tailings using wheat straw pyrolysis

Lihui Gao<sup>1</sup> · Lizhang Wang<sup>1</sup> · Shulei Li<sup>2</sup> · Yijun Cao<sup>2,3</sup>

Received: 29 April 2021 / Accepted: 19 October 2021 / Published online: 10 January 2022  
© Springer-Verlag GmbH Germany, part of Springer Nature 2021

## Abstract

The pollutants degradation rate of iron ore tailings-based heterogeneous catalysts is the main factor limiting its application. Herein, an iron ore tailings-based Fenton-like catalyst (I/W(3:1)-900-60) with a relatively fast catalysis rate was constructed by co-pyrolysis (900°C, 60 min holding time) of iron ore tailings and wheat straw with a mass ratio of 3:1. With wheat straw blending, the generated I/W(3:1)-900-60 presented a larger surface area (24.53 m<sup>2</sup>/g), smaller pore size (3.76 nm), reduced iron species (Fe<sup>2+</sup> from magnetic), and a higher catalytic activity (0.0229 min<sup>-1</sup>) than I-900-60 (1.32 m<sup>2</sup>/g, 12.87 nm, 0.012 min<sup>-1</sup>) pyrolyzed using single iron ore tailing under the same pyrolysis conditions. In addition, biochar and iron ore tailings in I/W(3:1)-900-60 were tightly combined through chemical bonding. The optimal catalyst remains active after three cycles, indicating its catalytic stability and recyclability. The good Fenton-like methylene blue degradation efficiency of I/W(3:1)-900-60 was ascribed to the sacrificial role of biochar, as well as the electron transfer between biochar and iron active sites or the redox cycles of  $\equiv\text{Fe}^{3+}/\text{Fe}^{2+}$ . This finding provides a facile construction strategy for highly active iron ore tailings-based Fenton-like catalyst and thereby had a great potential application in wastewater treatment.

**Keywords** Iron ore tailings · Wheat straw · Heterogeneous catalyst · Biochar · Decomposition rate

## Introduction

The mining industry is an important activity to extract mineral products around the world. Nevertheless, the mining process always brings a certain degree of pollution. Tailings are solid waste remaining after mining valuable minerals, which are usually disposed of at waste dams or landfills that present potential environmental damage (Rico et al. 2008;

Kossoff et al. 2014). In March 2020, a miserable accident involving a waste dam occurred when the Yichun waste dam (Harbin, China) for the storage of iron ore tailings collapsed. This accident caused 60,000 m<sup>3</sup> of mining tailings disclosing and 3 million m<sup>3</sup> of wastewater releasing, leading to 70 km of river pollution and serious economic loss. A number of other tailings dam accidents have occurred in different countries (Batista et al. 2020). According to statistics (Yi et al. 2020), the accumulated tailings were about 207 billion tons in China, of which the total amount of tailings produced in 2018 was about 12.11 billion tons. Among all types of tailings, iron ore tailings have the largest amount of production, about 4.76 billion tons, accounting for about 39.31% of the total tailings production (Huang et al. 2020).

Therefore, it is imperative to explore new technologies for reducing iron ore tailings and their reuse as raw materials to produce value-added products. Recently, a promising application of iron ore tailings has been utilized as adsorbents or catalysts to remove dye compounds (Silva et al. 2011; Augusto et al. 2018), e.g., as raw/regenerated efficient Fenton and Fenton-like catalysts for wastewater treatment. Given the high-iron contents observed in iron ore tailing, it is reasonable to assume that these wastes are good catalysts

Responsible Editor: Ricardo A. Torres-Palma

✉ Shulei Li  
lishuleibgs@163.com

✉ Yijun Cao  
yijuncao@126.com

<sup>1</sup> School of Environment and Spatial Informatics, China University of Mining and Technology, Xuzhou 221116, China

<sup>2</sup> National Engineering Research Center of Coal Preparation and Purification, China University of Mining and Technology, Xuzhou 221116, China

<sup>3</sup> School of Chemical Engineering and Technology, Zhengzhou University, Zhengzhou 450001, China

for Fenton or Fenton-like processes (Augusto et al. 2018). However,  $\text{Fe}^{2+}$  is the effective state for activating the oxidant, while the most common state in iron waste is  $\text{Fe}^{3+}$  (dos Santos et al. 2016), and the presence of  $\text{Fe}^{3+}$  modifies the degradation rate (reaction time as long as 24 h) of substance. Some researchers got significant progress in trying to enhance the pollutant oxidation rate through reducing  $\text{Fe}^{3+}$  to  $\text{Fe}^{2+}$  (Augusto et al. 2018; de Freitas et al. 2019). Freitas *et al.* achieved good results (80% dye decomposed with 3 h reaction) for the oxidation of methylene blue when iron ore tailing pretreated in a  $\text{CH}_4$  atmosphere at 550°C for 2 h.

Better degradation results could be achieved in the case of iron waste pretreatment under a reducing atmosphere ( $\text{H}_2$ ,  $\text{CO}$ ,  $\text{CH}_4$ ). Biomass could produce reducing gases and compounds during pyrolysis (Williams and Besler 1996; Wang et al. 2010). In our previous paper, we found that a unite mass wheat straw could produce about 5 mg/g  $\text{H}_2$  and 18 mg/g  $\text{CH}_4$  (Gao and Goldfarb 2019). Therefore, if iron tailings and wheat straw blends were pretreated through pyrolysis to realize the conversion of ferric iron to a low-valent state, it would not only improve the catalytic oxidation efficiency of organic matter but also realize the resource utilization of wheat straw, which is of great significance. Therefore, this paper applies methylene blue (MB) as a model pollutant to investigate the influence of pyrolysis conditions on the catalyzed degradation rate of pollutants. The pyrolyzed products' morphology, physical–chemical properties, stability, and catalytic mechanism were discussed. The research in this article aims to provide a theoretical basis for iron ore tailing catalysts with high degradation rates.

## Materials and methods

### Materials

Iron ore tailings were kindly provided by the “Hainan’s mining” industry, located in Hainan, China. The sample was hematite tailings (I) and ground to 74  $\mu\text{m}$  prior to use. Wheat straw was selected as biomass because of the high production in China, which was ground in a coffee mill and sieved to a particle size between 100 and 300  $\mu\text{m}$  (Gao and Goldfarb 2019). Supplementary Table S1 showed the characteristics of wheat straw and hematite tailings. MB was purchased from Aladdin Chemical Reagent Co., Ltd., China.

### Synthesis of the catalysts

Hematite tailings and wheat straw mixed with mass ratio 1:1, 2:1, 3:1, 4:1, and 5:1. Then, these mixtures were treated in a tube furnace using a heating rate of 10°C/min (Wang *et al.* found feedstock pyrolyzed at this heating rate could produce more reducing gas, such as  $\text{CO}$  and  $\text{H}_2$ )

(Wang et al. 2018) until different temperatures (while we do not have the ability to pyrolyze biochar at a temperature above 1000°C due to the furnace, so we selected the pyrolysis temperature as 500°C, 600°C, 700°C, 800°C, and 900) for different holding times (30 min, 45 min, 60 min, 90 min, and 120 min). The obtained catalyst was denoted as I/W(a:b)-T-t, where I is iron ore tailings, W is wheat straw, a:b is the mass ratio (w/w), T is the final temperature, and t is the holding time.

### MB decomposition experiments

To evaluate the decomposition rate of the catalyst produced from iron ore tailings, the bath catalytic experiments were carried out using 0.3 g of pyrolyzed product in contact with 100 mL dye solution with initial concentrations of 60 mg/L and 16 mmol  $\text{H}_2\text{O}_2$  under a shaker; 1.5 mL of solution was pipetted at given time intervals, centrifuged for 1 min, and the dye concentration ( $C$ ) was detected by a UV-vis spectrophotometer (Unico UV-2800) at 664 nm. A CTL-12 COD analyzer was applied for measuring the chemical demand oxygen (COD) of the sample catalyzed by I/W(3:1)-900-60 in the optimal pH value Fenton system. All tests were performed in triplicate, the degradation rate ( $k_t$ ) and the  $C/C_0$  at different degradation times for each sample were calculated, and then the results were expressed as mean  $\pm$  standard deviation.

To investigate the stability and reusability of catalyst, the optimal pyrolyzed product was reused/recycled four times for the MB decomposition under the same Fenton-like condition.

### Analytical method

The phase transformation of the ferrochemical group in pyrolyzed solid was analyzed by X-ray diffraction (XRD; Bruker D8 Advance, Germany). The morphology and composition were characterized by scanning electron microscopy and energy dispersive X-ray spectrometer (SEM-EDX; FEI QuantaTM 250, USA). The textural properties were tested by Brunauer–Emmett–Teller measurement (BET; BELSORP-max, Japan). The functional groups of catalysts were investigated by Fourier transform infrared spectroscopy (FTIR; Bruker Vertex 80v, Germany). Electron paramagnetic resonance (EPR; Bruker 300E spectrometer, Germany) was applied to test the main reactive oxidative species (ROS) generated in the system. Fe valence and carbon functional group variation of catalysts were characterized by X-ray photoelectron spectroscopy (XPS; Thermo Fisher Escalab 250 Xi, USA), and the  $\text{C}1s_{1/2}$ (284.6 eV) was used as the binding energy calibration standard.

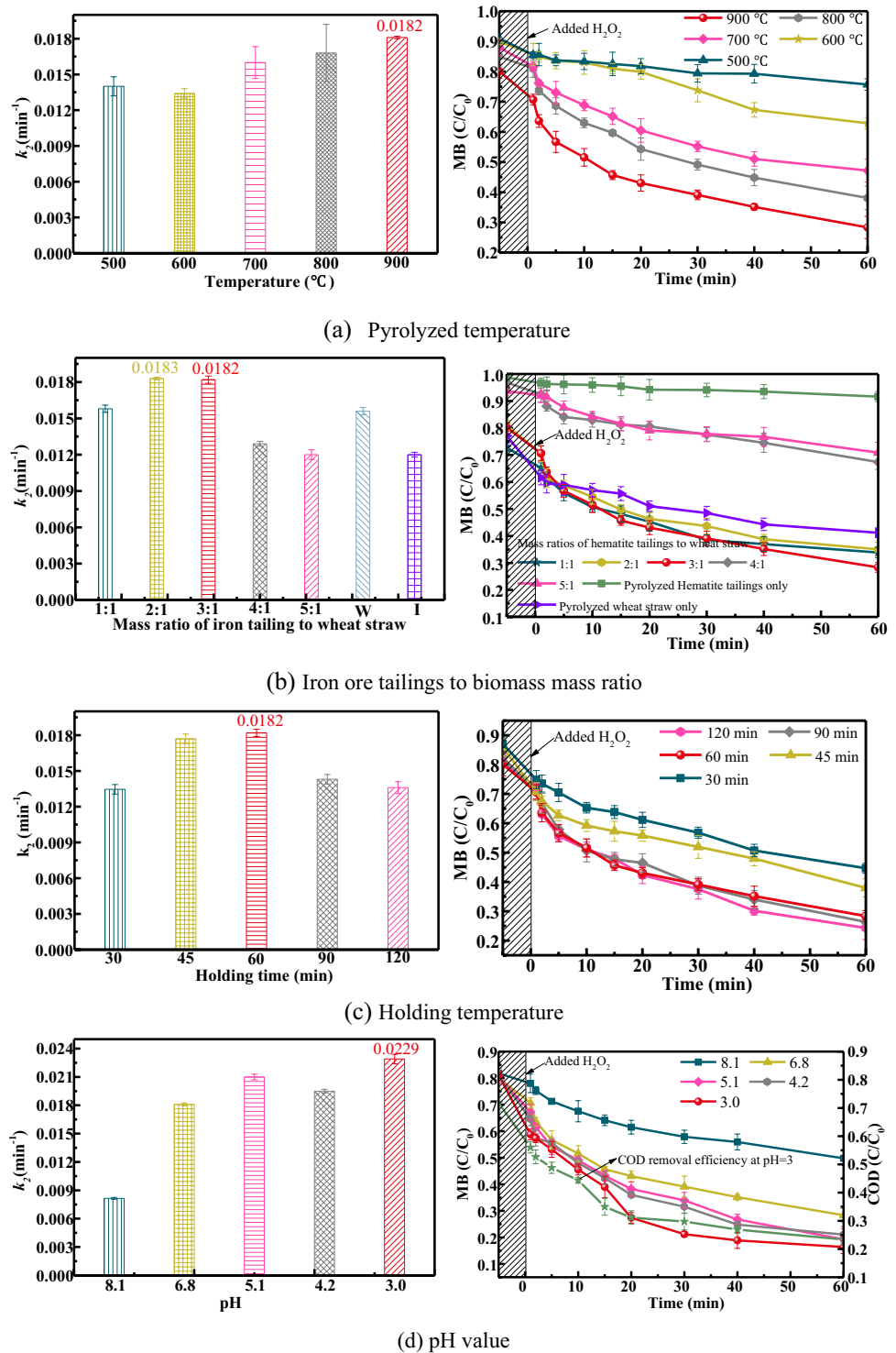
## Results and discussion

### Determination of optimal pyrolysis based on degradation rate

The pyrolysis preparation mass ratio (iron ore tailings to wheat straw), reaction time, and heating rate were fixed

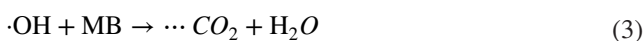
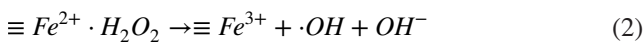
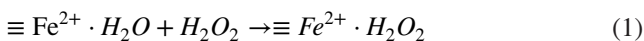
at 3:1, 60 min, and 10°C/min, respectively, and catalysts were obtained under different pyrolysis temperatures. Figure 1(a) showed the comparison of MB removal efficiency versus time and pseudo-second-order kinetic constant ( $k_2$ ,  $R^2 > 0.994$ ) under different catalysts, in which -5 min means that the  $H_2O_2$  was added after 5-min adsorption. Only approximately 20% of MB was removed after 1 h

Fig. 1 Degradation of MB by pyrolyzed product prepared under different conditions

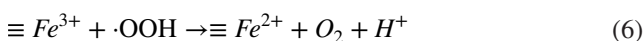
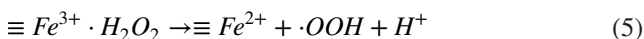
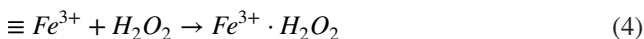


with a kinetic rate of  $0.0139 \text{ min}^{-1}$  when the product prepared at  $500^\circ\text{C}$  was used. However, the removal rate and efficiency were substantially improved as the pyrolyzed temperature increased. The best decomposition rate ( $0.0182 \text{ min}^{-1}$ ) and efficiency (74%) were reached using a catalyst prepared at  $900^\circ\text{C}$ , which was much higher than the generated iron ore tailings catalyst reported by Augusto *et al.* ( $7.4 \times 10^{-4} \text{ min}^{-1}$ , 63%) (Augusto *et al.* 2018). Considering the dye decomposition rate and efficiency, the optimal pyrolysis temperature for synthesizing catalyst was determined to be  $900^\circ\text{C}$ .

Setting the pyrolysis temperature at  $900^\circ\text{C}$ , the final holding time at 60 min, and the heating rate at  $10^\circ\text{C}/\text{min}$ , the removal efficiency and rate of MB were investigated by pyrolysis products at different mass ratios. As shown in Fig. 1(b), only 10% MB was removed with a removal rate  $k_2$  of  $0.0120 \text{ min}^{-1}$  when the catalyst was prepared by hematite tailings only, indicating that the pyrolyzed product synthesized from iron ore tailings might not be active for dye degradation. While the decomposition efficiency of MB ( $k_2$  increased from 0.0120 to  $0.0182/0.0183 \text{ min}^{-1}$ ) gradually increased when the products made from hematite tailings and wheat straw blends were used as a catalyst. This may be due to biomass blends that helped to reduce the  $\equiv\text{Fe}^{3+}$  to  $\equiv\text{Fe}^{2+}$  or low-valent iron (Ellison and Boldor 2021). The mechanism of  $\text{H}_2\text{O}_2$  activation by iron ore tailings-based catalyst with  $\equiv\text{Fe}^{2+}$  may involve the following reaction processes (Luo *et al.* 2010). Firstly, a complex assigned as  $\equiv\text{Fe}^{2+} \cdot \text{H}_2\text{O}_2$  may form between the hydrous surface of  $\equiv\text{Fe}^{2+} \cdot \text{H}_2\text{O}$  and  $\text{H}_2\text{O}_2$  (Eq. (1)), where  $\equiv\text{Fe}^{2+} \cdot \text{H}_2\text{O}$  represents the reduced sites on the iron ore tailings catalyst surface. The formed  $\equiv\text{Fe}^{2+} \cdot \text{H}_2\text{O}_2$  can produce  $\cdot\text{OH}$  by  $\text{H}_2\text{O}_2$  activation, which is ready to decompose and oxidize MB (Eqs. (2) and (3)).



However, the radical formation mechanism by  $\equiv\text{Fe}^{3+}$  and  $\text{H}_2\text{O}_2$  is proposed as follows:

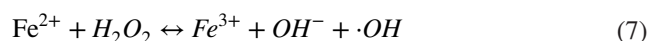


The formed  $\equiv\text{Fe}^{2+}$  subsequently produces  $\cdot\text{OH}$  (Eqs. (1)–(3)). Although  $\cdot\text{OH}$  can be generated from  $\text{H}_2\text{O}_2$  when

either  $\equiv\text{Fe}^{2+}$  or  $\equiv\text{Fe}^{3+}$  is present, the generation rates are much faster between  $\equiv\text{Fe}^{2+}$  and oxidant (Kwan and Voelker 2002). Although the degradation efficiency for catalysts produced from mass ratio 1:1, 2:1, and 3:1 was equivalent, degradation rate  $k_2$  values of mass ratio 3:1 ( $0.0182 \text{ min}^{-1}$ ) and 2:1 ( $0.0183 \text{ min}^{-1}$ ) were higher than 1:1 ( $0.0158 \text{ min}^{-1}$ ). In order to realize the iron ore tailings bulk utilization and construct a catalyst with a higher degradation rate, we determined that the optimal mass ratio of iron ore tailings to wheat straw was 3:1.

Fixing the pyrolysis temperature at  $900^\circ\text{C}$ , the ratio of iron ore tailings to wheat straw at 3:1, and the heating rate at  $10^\circ\text{C}/\text{min}$ , the optimum holding time was investigated in Fig. 1(c). The dye decomposition efficiency of the pyrolyzed product was enhanced when the holding time for the synthesis catalyst stretched from 30 to 60 min. However, the degradation efficiency of MB was not significantly improved when the holding time was further extended to 90 min and 120 min. Interestingly,  $k_2$  showed a first increasing then decreasing trend as the holding time extended and reached the maximum ( $0.0182 \text{ min}^{-1}$ ) when the holding time was 60 min. Thus, 60 min was the optimal catalyst holding time among those investigated parameters.

To sum up, the relative optimal pyrolysis condition was a blends ratio of 3:1, a pyrolysis temperature of  $900^\circ\text{C}$ , and a holding time of 45 min. pH as an important factor for the efficiency of Fenton-like reaction, the effect of pH was investigated in Fig. 1(d). We could see that pH could significantly affect the degradation of MB in iron ore tailings-catalyzed Fenton-like process. As shown in Fig. 1(d), the degradation efficiency was relatively low and the  $k_2$  values were  $0.0104 \text{ min}^{-1}$  and  $0.0182 \text{ min}^{-1}$  at pH 8.1 and 6.8 (did not adjust). While the decomposition of MB gradually increased as the pH value decreased and got the highest/fastest degradation efficiency (84% MB removal,  $0.0229 \text{ min}^{-1}$ ) at around pH 3, which was consistent with previous studies (Hu *et al.* 2011). The generation of  $\cdot\text{OH}$  from  $\text{H}_2\text{O}_2$  is the key step in the entire Fenton-like process, and  $\cdot\text{OH}$  catalyzed by iron ore tailings are gradually limited with pH increasing. The higher pH with more  $\text{OH}^-$  will cause the reaction (Eq. (7)) to shift back and reduce the activity of the Fenton reagent (Zheng *et al.* 2016), which resulted in a slow decomposition rate of I/W(3:1)-900-60. Meanwhile, the COD removal efficiency of I/W(3:1)-900-60 at pH = 3 was shown in Fig. 1(d), and the COD removal efficiency was 76.6% after 60 min (from 141.2 to 32.3 mg/L). Therefore, the heterogeneous reaction with I/W(3:1)-900-60 as the catalyst can not only attack the MB chromophore group but also realize the degradation and mineralization of organic matter.





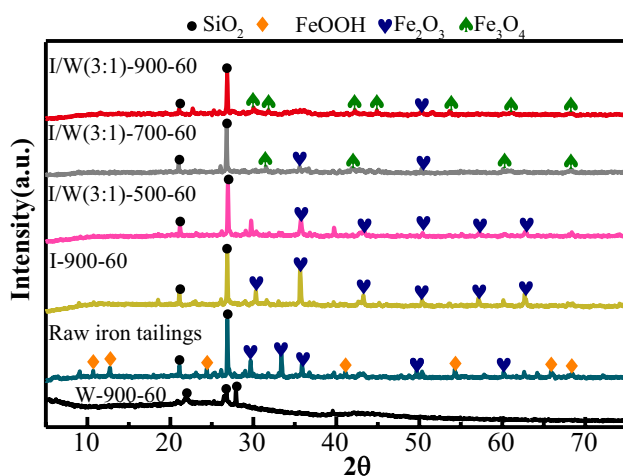


Fig. 2 XRD patterns of the raw and prepared samples

### Catalyst characterization

Since the catalytic efficiency was apparently different by I-900-60, W-900-60, and I/W(3:1)-900-60, XRD patterns were collected to indicate the phase information of these samples shown in Fig. 2. The XRD pattern of I/W(3:1)-900-60 showed diffraction peaks at  $2\theta=30.3^\circ$ ,  $43.3^\circ$ ,  $53.8^\circ$ ,  $57.5^\circ$ ,  $68.2^\circ$  corresponded to  $\text{Fe}_3\text{O}_4$ , which exhibits magnetic characteristics. The peaks of W-900-60 were noted at  $2\theta = 21.8^\circ$ ,  $26.5^\circ$ ,  $28.0^\circ$ , corresponding to  $\text{SiO}_2$  crystallites. The diffraction peaks of raw iron ore tailings were attributed to  $\alpha\text{-FeOOH}$ , and  $\alpha\text{-FeOOH}$  was converted to  $\text{Fe}_2\text{O}_3$  when heated to  $900^\circ\text{C}$  under  $\text{N}_2$  atmosphere (Zhang et al. 2018). Therefore, only the pyrolysis of iron ore tailings or wheat straw cannot produce a composite with low-valent iron.

Significant transformation of  $\text{Fe}_2\text{O}_3$  to  $\text{Fe}_3\text{O}_4$  was observed at  $700\text{--}900^\circ\text{C}$ . When the temperature reached above  $700^\circ\text{C}$ , most of the  $\text{Fe}_2\text{O}_3$  peaks disappeared and the diffraction peaks of magnetite appeared. It can be concluded that  $\text{Fe}_2\text{O}_3$  with trivalent could be reduced to  $\text{Fe}_3\text{O}_4$  during high-temperature pyrolysis. More  $\text{Fe}_2\text{O}_3$  spindles were converted to  $\text{Fe}_3\text{O}_4$  as the temperature increased. This is due to that there were organic matters such as cellulose, hemicellulose, and lignin in wheat straw, and these organic matters could be cracked and devolatilized into reducing gas or liquid, such as  $\text{H}_2$ ,  $\text{CH}_4$ . In our previous study, we noted that wheat straw could devolatilize  $2.1 \text{ mg/g}_{\text{ws}} \text{H}_2$  and  $15.7 \text{ mg/g}_{\text{ws}} \text{CH}_4$  at a temperature of  $650^\circ\text{C}$ . Meanwhile, the rate of devolatilization and the amount of thermal creaking gas increase as the temperature increases (Gao and Goldfarb 2019). In addition, some literature reported that pyrolyzed gases could lead to a ferric iron reduction (Gong et al. 2012; Sharma et al. 2015; Pang et al. 2019; Xun et al. 2019). In summary, in the process of co-pyrolysis of wheat straw and

iron ore tailings, the reducing substances such as  $\text{H}_2$  or  $\text{CH}_4$  produced from wheat straw exhibited strong reducibility to reduce iron ore tailings to magnetite. Furthermore, the reduction degree increased as the pyrolysis temperature increased.

To illustrate the effect of biomass/wheat straw on the high degradation efficiency catalyst formation, the morphologies of I-900-60 and I/W(3:1)-900-60 were further compared. The surface morphologies of I-900-60 and I/W(3:1)-900-60 were shown in Supplementary Fig.S1. The I-900-60 presented a large flaky structure with a flat and non-porous surface after pyrolysis, mainly because of the natural structure of iron ore tailings. In the case of I/W(3:1)-900-60, SEM images showed that most particles had a smaller flake structure with porous surfaces. This result indicated that mixing wheat straw promotes the formation of a porous and smaller flake structure.

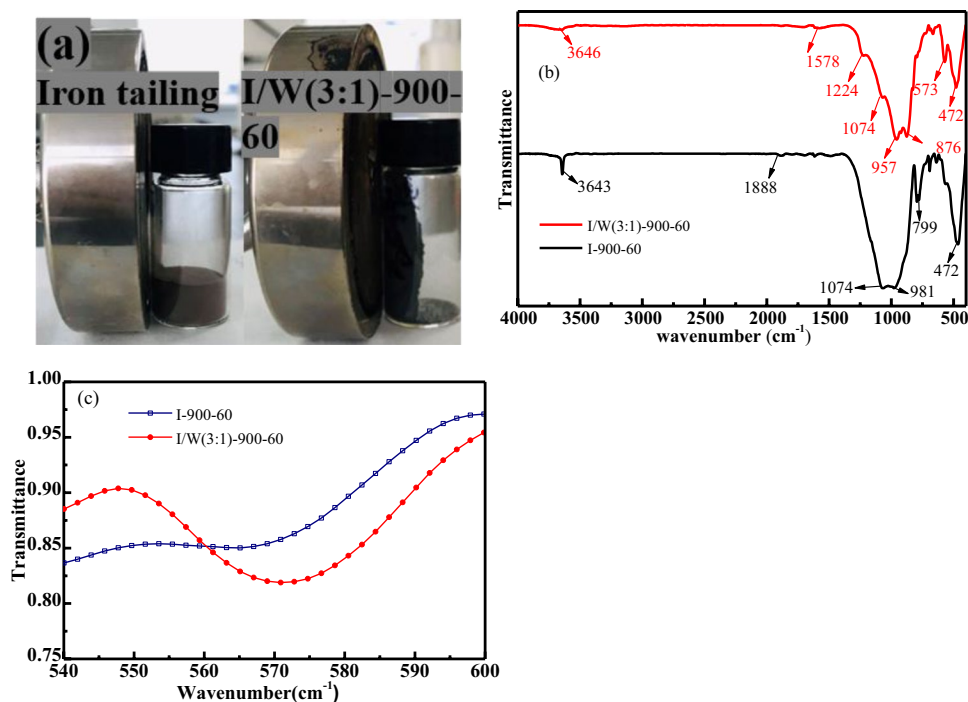
As observed from SEM images, I/W(3:1)-900-60 had a smaller particle than I-900-60.  $\text{N}_2$  adsorption–desorption isotherm was applied to calculate the surface area, pore volume, and pore size distribution. As shown in Table 1 and Supplementary Fig. S2, the average pore sizes of I-900-60 and I/W(3:1)-900-60 were 12.87 nm and 3.76 nm. However, the total pore volumes were  $0.00387 \text{ cm}^3/\text{g}$  and  $0.0225 \text{ cm}^3/\text{g}$ , respectively. Thus, we can conclude that wheat straw addition increased the pore volume and decreased the average pore size. Additionally, although I/W(3:1)-900-60 had a much larger specific surface area ( $24.53 \text{ m}^2/\text{g}$ ) than I-900-60 ( $1.32 \text{ m}^2/\text{g}$ ), its surface area was smaller than those reported iron-load-activated carbon adsorbent ( $300\text{--}600 \text{ m}^2/\text{g}$ ) (Park et al. 2015; He et al. 2016; Saleh et al. 2017). This result further verified that prepared catalysts from iron ore tailings had weak adsorption ability. Therefore, we speculated that MB degradation by I/W(3:1)-900-60 was due to catalysis instead of adsorption. I/W(3:1)-900-60, with relatively larger surface area and richer pore volume, could provide greater active catalysis sites and increase catalysis performance (Neamtu et al. 2004; Duarte et al. 2012), agreed with the improved MB degradation efficiency catalyzed by I/W(3:1)-900-60.

There is an important question to further discuss that whether composites (wheat straw biochar and iron ore tailings) were simply mixed and exist alone or integrated

Table 1 BET and BJH results of prepared catalysts

Samples	Surface area ( $\text{m}^2/\text{g}$ )	Pore volume ( $\text{cm}^3/\text{g}$ )	Average pore size (nm)
I-900-60	1.32	0.00387	12.87
I/W(3:1)-900-60	24.53	0.0225	3.76

**Fig. 3** (a) The photos of the products attraction to a magnetic device; (b) FTIR spectra of I-900-60 and I/W(3:1)-900-60 in the wavenumber range between 4000 and 400  $\text{cm}^{-1}$ ; (c) zoomed FTIR spectra in the wavenumber range between 540 and 600  $\text{cm}^{-1}$

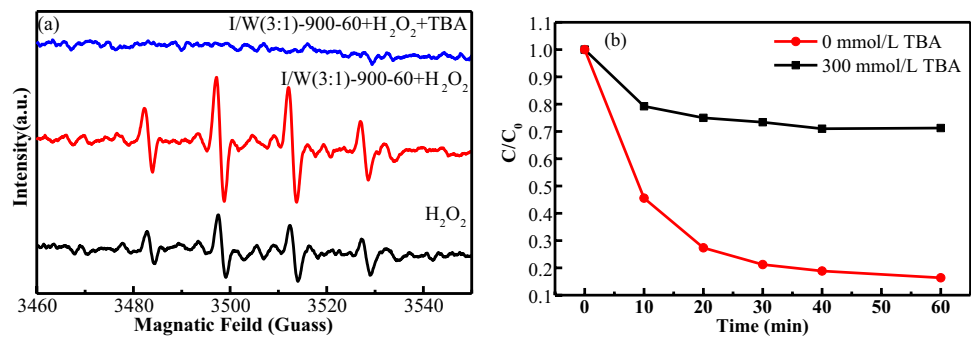


together. Figure 3(a) showed that the catalysts were attracted as a whole by a magnetic device, indicating iron ore tailings and biochar combined as a whole. This binding form is beneficial to remove the catalyst from wastewater after the reaction. In addition, FTIR spectra in the wavenumber range between 4000 and 400  $\text{cm}^{-1}$  were shown in Fig. 3(b). The peak at 3643/3646  $\text{cm}^{-1}$  was attributed to O-H stretching and bending vibrations (Zhang et al. 2018). Similar peaks were observed in the spectra of both I-900-60 and I/W(3:1)-900-60, including Si-O stretching vibrations of the Si-O-Si, Si-O-Al, and Si-O-Fe groups (1074  $\text{cm}^{-1}$ , 957/981  $\text{cm}^{-1}$ , 472  $\text{cm}^{-1}$ ), although their intensities varied (Doelsch et al. 2003). The silicon content in iron ore tailings was much higher than that in wheat straw (Supplementary Table S1). Therefore, the intensity of Si-O stretching vibration in I-900-60 was stronger than in the spectrum of I/W(3:1)-900-60. Meanwhile, new peaks associated with the -C=O and -C-H stretching vibration at 1224  $\text{cm}^{-1}$  and 876  $\text{cm}^{-1}$  were observed in the spectrum of I/W(3:1)-900-60; these peaks were assigned mainly to the formed biochar that has the corresponding groups, such as carboxyl and ester groups. In addition, as shown in Fig. 3(c), a new peak at 573  $\text{cm}^{-1}$  attributed to an asymmetric Fe-O stretching vibration was observed. It might be caused by loading iron into biochar or  $\text{Fe}_3\text{O}_4$  itself (Yuan and Dai 2014). Therefore, the new bond Fe-O on I/W(3:1)-900-60 may indicate the combination of iron and biochar that occurred through chemical bonds.

### The catalyst's stability and reusability analysis

It is important to evaluate the stability of a heterogeneous catalyst. As illustrated in Supplementary Fig. S3, I/W(3:1)-900-60 was stable in the first three runs and remained high MB degradation efficiency. At the 4th run, the activity of I/W(3:1)-900-60 reduced slightly, but the degradation efficiency is still higher than 80%, showing that the iron ore tailings-based catalyst can be reused for at least 4 Fenton-like cycles without significant activity loss. This slight activity loss is probably due to the small molecules produced during MB degradation occupying part of the active sites, leading to a decrease in catalytic efficiency (Zhang et al. 2018). In addition, the concentration of leaching iron ions after the first three runs was measured. As shown in Supplementary Table S2, the concentrations of leached iron were 0.089 mg/L, 0.085 mg/L, and 0.093 mg/L, which were only 0.8% of the iron content in I/W(3:1)-900-60. Low-leached iron concentration also indicated that heterogeneous Fenton catalysis was the dominant reaction for MB removal (Gao et al. 2017). Meanwhile, XRD and SEM were applied to examine the structural stability of I/W(3:1)-900-60. As illustrated in Supplementary Fig. S4, compared with fresh catalyst, the crystalline nature and morphology of used I/W(3:1)-900-60 did not change significantly. These results indicated that the cost-effective I/W(3:1)-900-60 was a promising heterogeneous catalyst in Fenton-like catalytic degradation of organic wastewater due to its significant stability and reusability.

**Fig. 4** (a) DMPO-ROS adducts generated from I/W(3:1)-900-60 Fenton catalysis reactions at 10 min. (b) Influence of radical scavenger (TBA) on the catalytic degradation of MB



## Reactive oxidative species and catalysis mechanism

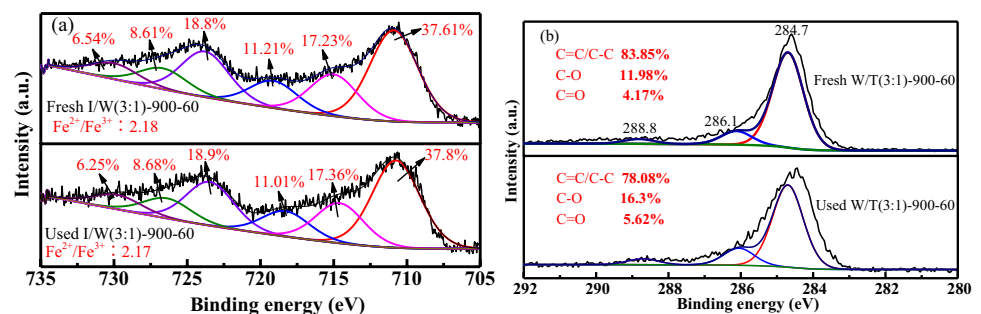
ROS produced in I/W(3:1)-900-60 was detected by an EPR spin-trap technique with DMPO. Figure 4(a) showed the EPR spectrum of the generated adducts during the 10-min reaction. On the EPR spectrum, there was observed a four-fold peak with an intensity of 1:2:2:1, which was labeled to the DMPO-OH (Yang et al. 2013). However, the four-fold peak has not appeared in the presence of 300 mmol/L T-Butyl alcohol (TBA, OH scavenger). Therefore, OH was the key ROS produced in I/W(3:1)-900-60 catalyzed Fenton-like reactions. Figure 4(b) showed the effect of ·OH on MB degradation. We can see the removal efficiency of MB significantly decreased from 84 to 29% in the presence of 300 mmol/L. This result indicated that ·OH played a dominant role in MB degradation in I/W(3:1)-900-60 catalyzed Fenton-like reactions.

The electron exchange between Fe(II)/Fe(III) and H<sub>2</sub>O<sub>2</sub> can induce the formation of ·OH in the heterogeneous Fenton-like reaction. XPS was applied to analyze the chemical state of iron species on I/W(3:1)-900-60 before and after the catalysis reaction. Figure 5 shows XPS results of Fe 2*p* in fresh and used I/W(3:1)-900-60. The peaks located at 724.8 eV and 710.9 eV were attributed to Fe 2*p*<sub>1/2</sub> and Fe 2*p*<sub>3/2</sub> states of Fe 2*p* orbitals, respectively (Gao et al. 2017; Li et al. 2018). Furthermore, the Gaussian-Lorentzian was applied to decompose these two peaks into 6 different fitting peaks (Ding et al. 2016). Among them, the fitting peaks located at 719.1 eV and 729.9 eV attribute to satellite peaks, as well as at 712.0 eV and 725.3 eV assign to Fe<sup>3+</sup>, and at 710.6

eV and 723.8 eV correspond to Fe<sup>2+</sup>, respectively (Li et al. 2018). A summary of deconvoluted peaks' area and the Fe<sup>2+</sup>/Fe<sup>3+</sup> ratio was presented in Fig. 5(a). Apparently, the ratio value of Fe<sup>2+</sup>/Fe<sup>3+</sup> decreased from 2.18 to 2.17 after the reaction, demonstrating only a small amount of ≡Fe<sup>2+</sup> lost electrons and oxidized to ≡Fe<sup>3+</sup> during the catalysis reaction. These XPS results are in accordance with the good recyclability and stability of I/W(3:1)-900-60 catalyst, which may attribute to the protective effects of the biochar (Li et al. 2018).

To further verify the protective role of biochar during Fenton-like reaction. XPS analysis was conducted to investigate the functional groups' changes of I/W(3:1)-900-60 catalyst. As illustrated in Fig. 5(b), the C1s spectra can be decomposed into three fitting peaks with C=C sp<sup>2</sup>/C-Csp<sup>3</sup> (284.7 eV), C-O (286.1 eV), and C=O (288.8 eV) (Li et al. 2017b). Apparently, compared with the fresh I/W(3:1)-900-60, the relative content of C=C sp<sup>2</sup>/C-Csp<sup>3</sup> carbon was reduced by 5.8% and C-O and C=O increased by 4.4% and 1.4% after catalysis reaction. This indicates that biochar was oxidized during the Fenton-like process with turning C=C sp<sup>2</sup>/C-Csp<sup>3</sup> carbon to C-O or C=O. Therefore, the recyclability and stability of the I/W(3:1)-900-60 catalyst may owe to the existence of biochar which acted as a sacrificial role and limited the oxidation of iron active sites in the catalyst. Actually, the biochar can act as a catalyst with electron donor-accepter for the induction of H<sub>2</sub>O<sub>2</sub> into ·OH or ·OOH. The persistent free radicals (PFRs) on the surface of biochar formed by the thermal decomposition of organic compounds can be the reduced and oxidized active sites through electron

**Fig. 5** XPS spectra of Fe 2*p* (a) and C1s (b) on I/W(3:1)-900-60 before and after catalysis reaction



transfer to form radical species ((Khachatryan and Dellinger 2011; Zhu et al. 2018). Fang *et al.* found that PFRs on the surface of biochar have an important influence on the production of  $\bullet\text{OH}$  by  $\text{H}_2\text{O}_2$  activation (Fang et al. 2014). In addition, the PFRs on the biochar surface lead to the existence of unpaired electrons, which can exchange electrons directly with organic matter, accelerating the MB degradation efficiency (Fang et al. 2013; Yang et al. 2016).

According to the above analysis results and discussion, the possible Fenton-like reaction mechanism was illustrated in Fig. 6. In the beginning, the MB molecules were

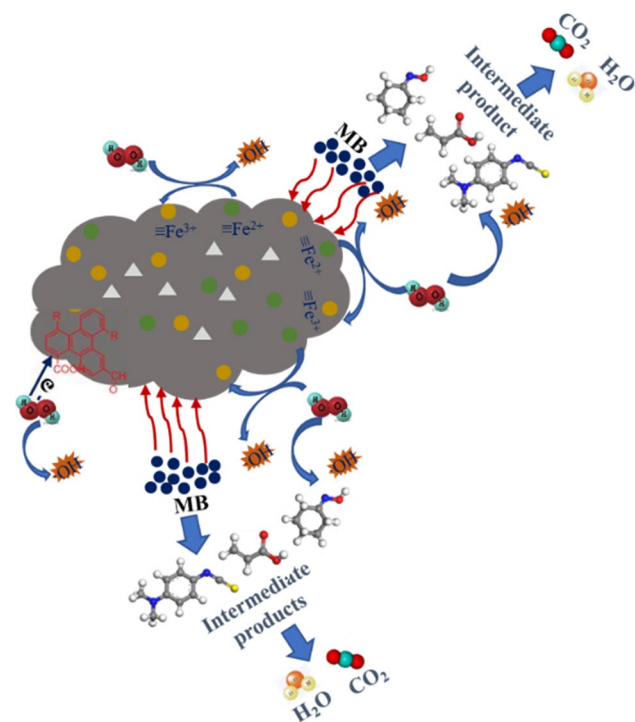


**Fig. 6** Proposed mechanism for Fenton catalysis reaction of I/W(3:1)-900-60

adsorbed onto biochar of I/W(3:1)-900-60 from aqueous solution through surface action and pore diffusion. Then, the iron active sites of  $\equiv\text{Fe}^{2+}$  and PFRs in biochar simultaneously transfer an electron to  $\text{H}_2\text{O}_2$  to generate  $\bullet\text{OH}$  for MB degradation. According to the previous research (Zhang et al. 2018), the degradation process of MB can be described as that under the bombardment of  $\bullet\text{OH}$ , the N-C<sub>5</sub>H<sub>5</sub> and S-C<sub>5</sub>H<sub>5</sub> on the MB molecule is first broken and formed 4-(N,N-dimethylamino) phenyl isothiocyanate. Secondly,  $\bullet\text{OH}$  radicals combined with aromatic rings to form monocyclic aromatic intermediates through hydroxylation and oxidation reactions. Finally, ring-opening products, such as methyl methacrylate and isopropyl methyl ketone, were produced and then mineralized into  $\text{CO}_2$  and  $\text{H}_2\text{O}$ . Moreover, the electron transfer between PFRs and iron active sites or the redox cycles of  $\equiv\text{Fe}^{3+}/\text{Fe}^{2+}$  combined results in the enhanced degradation efficiency and rate of heterogeneous Fenton-like reaction. Significantly, the stable performance of I/W(3:1)-900-60 with good reusability is due to the sacrificial effect of biochar for limiting the oxidation of iron active sites. In addition, the presence of unpaired electrons in PFRs contributes to a certain extent to improve the degradation efficiency of pollutants.

Table 2 showed the MB decompose rate  $k_2$  for various Fenton-like catalysts. We can see that I/W(3:1)-900-60 ( $0.0229 \text{ min}^{-1}$ ) exhibited a higher  $k_2$  than or comparable to most reported kinetic rate data, which indicates that the co-pyrolysis of iron ore tailings and biomass waste is an effective way to improve the degradation rate/efficiency of iron ore tailings-based heterogeneous catalysts. Meanwhile, it is of great significance to realize the resource utilization of iron ore tailings. However, these kinetic rate dates are far less than the degradation rate of homogeneous Fenton catalysis (Gou et al. 2021). Thus, the performance optimization of iron ore tailings-based heterogeneous catalysts based on porous and low-valent iron still needs further study.

**Table 2** Comparison of MB removal by Fenton-like methods with different catalysts

Catalyst	MB (mg/L)	Catalyst dosage (g/L)	Time (min)	$k$ ( $\text{min}^{-1}$ )	Reference
I/W(3:1)-900-60	60	3	60	$2.29 \times 10^{-2}$	This study
$\text{Fe}_3\text{O}_4$	100	3	30	$1 \times 10^{-3}$	Costa et al. 2008
$\text{Fe}_3\text{O}_4/\text{H}_2/300/1\text{h}$	100	3	30	$4 \times 10^{-3}$	Costa et al. 2008
$\text{Fe}_3\text{O}_4/\text{H}_2/400/1\text{h}$	100	3	30	$2 \times 10^{-2}$	Costa et al. 2008
Ferrocene	10	0.372	120	$6.17 \times 10^{-3}$	Wang et al. 2014
$\text{Fe}_3\text{O}_4/\text{rGO}$	10	0.3	120	$2.6 \times 10^{-3}$	Liu et al. 2013
$\text{Fe}_3\text{O}_4/\text{SiO}_2/\text{C}$	50	1	140	$3.6 \times 10^{-2}$	Liu et al. 2013
$\text{Fe}_3\text{O}_4/\text{CeO}_2$	100	1	120	$2 \times 10^{-2}$	Li et al. 2017a
$\text{Fe}_3\text{O}_4/\text{galic acid}/\text{GO}$	64	1	200	$1.2 \times 10^{-2}$	Hua et al. 2017
N,C/CuO- $\text{Fe}_2\text{O}_3$	75	0.1	180	$1.08 \times 10^{-2}$	Ren et al. 2019
FeNi/C-300	30	1	30	$1.05 \times 10^{-2}$	Li et al. 2020



## Conclusions

An iron ore tailings-based Fenton-like catalyst (I/W(3:1)-900-60) with a relatively fast catalysis rate was constructed by co-pyrolysis (900°C, 60 min holding time) of iron ore tailings and wheat straw with a mass ratio of 3:1. Compared with single pyrolyzed iron ore tailing, the catalytic efficiency and rate of I/W(3:1)-900-60 (0.0229 min<sup>-1</sup>, 84%) were considerably enhanced for the decomposition of MB due to the electron transfer between biochar and iron active sites or the redox cycles of  $\equiv\text{Fe}^{3+}/\text{Fe}^{2+}$ . As a result of the sacrificial effect of biochar, oxidizing C=Csp<sup>2</sup> bonds and limiting the deactivation of iron active sites ( $\equiv\text{Fe}^{2+}$ ), I/W(3:1)-900-60 showed good reusability and stability. Moreover, the presence of unpaired electrons in persistent free radicals (PFRs) of biochar accelerated the electron exchange and further enhanced the MB decomposition rate. This work opens up a way to synthesize an iron ore tailings-based Fenton-like catalyst with a higher degradation rate as well as realize the utilization of solid wastes.

**Acknowledgements** The authors wish to express their regards to Ms. Jing Hou for her assistance during the COD measuring experiments.

**Author contribution** Lihui Gao: writing – original draft, methodology, data curation; Lizhang Wang: writing – reviewing and editing; Shulei Li: investigation, sample preparation; Yijun Cao: supervision and editing.

**Funding** L.Gao acknowledges the financial support of the National Natural Science Foundation of China (5210040121), the Jiangsu Provincial Natural Science Foundation of China (BK20210498), and the fellowship of China Postdoctoral Science Foundation (2021M693420).

**Availability of data and materials** All data generated or analyzed during this study are included in this published article.

## Declarations

**Ethics approval and consent to participate** Not applicable

**Consent for publication** Not applicable

**Competing interests** The authors declare no competing interests.

## References

- Augusto TDM, Chagas P, Sangiorgio DL, Mac Leod TCDO, Oliveira LCA, De Castro CS (2018) Iron ore tailings as catalysts for oxidation of the drug paracetamol and dyes by heterogeneous Fenton. *J Environ Chem Eng* 6:6545–6553. <https://doi.org/10.1016/j.jece.2018.09.052>
- Batista ÉR, Carneiro JJ, Araújo Pinto F, dos Santos JV, Carneiro MAC (2020) Environmental drivers of shifts on microbial traits in sites disturbed by a large-scale tailing dam collapse. *Sci Total Environ* 738:1–12. <https://doi.org/10.1016/j.scitotenv.2020.139453>
- Costa RCC, Moura FCC, Ardisson JD, Fabris JD, Lago RM (2008) Highly active heterogeneous Fenton-like systems based on Fe<sup>0</sup>/Fe<sub>3</sub>O<sub>4</sub> composites prepared by controlled reduction of iron oxides. *Appl Catal B Environ* 83:131–139
- de Freitas VAA, Breder SM, Silvas FPC, Radino Rouse P, de Oliveira LCA (2019) Use of iron ore tailing from tailing dam as catalyst in a Fenton-like process for methylene blue oxidation in continuous flow mode. *Chemosphere* 219:328–334. <https://doi.org/10.1016/j.chemosphere.2018.12.052>
- Ding C, Zeng Y, Cao L, Zhao L, Zhang Y (2016) Hierarchically porous Fe<sub>3</sub>O<sub>4</sub>/C nanocomposite microspheres via a CO<sub>2</sub> bubble-templated hydrothermal approach as high-rate and high-capacity anode materials for lithium-ion batteries. *J Mater Chem A* 4:5898–5908
- Doelsch E, Masion A, Rose J, Stone WEE, Bottero JY, Bertsch PM (2003) Chemistry and structure of colloids obtained by hydrolysis of Fe(III) in the presence of SiO<sub>4</sub> ligands. *Colloids Surf A Physicochem Eng Asp* 217:121–128. [https://doi.org/10.1016/S0927-7757\(02\)00566-6](https://doi.org/10.1016/S0927-7757(02)00566-6)
- dos Santos PL, Guimarães IR, Mesquita AM, Guerreiro MC (2016) Copper-doped akaganeite: application in catalytic Cupro-Fenton reactions for oxidation of methylene blue. *J Mol Catal A Chem* 424:194–202. <https://doi.org/10.1016/j.molcata.2016.08.034>
- Duarte F, Maldonado-Hódar FJ, Madeira LM (2012) Influence of the particle size of activated carbons on their performance as Fe supports for developing Fenton-like catalysts. *Ind Eng Chem Res* 51:9218–9226. <https://doi.org/10.1021/ie300167r>
- Ellison CR, Boldor D (2021) Mild upgrading of biomass pyrolysis vapors via ex-situ catalytic pyrolysis over an iron-montmorillonite catalyst. *Fuel* 291:120226. <https://doi.org/10.1016/j.fuel.2021.120226>
- Fang G, Gao J, Dionysiou DD, Liu C, Zhou D (2013) Activation of persulfate by quinones: free radical reactions and implication for the degradation of PCBs. *Environ Sci Technol* 47:4605–4611. <https://doi.org/10.1021/es400262n>
- Fang G, Gao J, Liu C, Dionysiou DD, Wang Y, Zhou D (2014) Key role of persistent free radicals in hydrogen peroxide activation by biochar: implications to organic contaminant degradation. *Environ Sci Technol* 48:1902–1910. <https://doi.org/10.1021/es4048126>
- Gao L, Goldfarb JL (2019) Solid waste to biofuels and heterogeneous sorbents via pyrolysis of wheat straw in the presence of fly ash as an in situ catalyst. *J Anal Appl Pyrolysis* 137:96–105. <https://doi.org/10.1016/j.jaap.2018.11.014>
- Gao C, Chen S, Quan X, Yu H, Zhang Y (2017) Enhanced Fenton-like catalysis by iron-based metal organic frameworks for degradation of organic pollutants. *J Catal* 356:125–132. <https://doi.org/10.1016/j.jcat.2017.09.015>
- Gong X, Guo Z, Wang Z (2012) Effects of Fe<sub>2</sub>O<sub>3</sub> on pyrolysis reactivity of demineralized higher rank coal and its char structure. *Ciesc J* 60:2321–2326. <https://doi.org/10.16552/j.cnki.issn1001-1625.2016.06.035>
- Gou Y, Chen P, Yang L, Li S, Peng L, Song S, Xu Y (2021) Degradation of fluoroquinolones in homogeneous and heterogeneous photo-Fenton processes: a review. *Chemosphere* 270:1–12. <https://doi.org/10.1016/j.chemosphere.2020.129481>
- He Q, Dai J, Zhu L, Xiao K, Yin Y (2016) Synthesis and lead absorption properties of sintered activated carbon supported zero-valent iron nanoparticle. *J Alloys Compd* 687:326–333. <https://doi.org/10.1016/j.jallcom.2016.06.139>
- Hu X, Liu B, Deng Y, Chen H, Luo S, Sun C, Yang P, Yang S (2011) Adsorption and heterogeneous Fenton degradation of 17 $\alpha$ -methyltestosterone on nano Fe<sub>3</sub>O<sub>4</sub>/MWCNTs in aqueous solution. *Appl Catal B Environ* 107:274–283. <https://doi.org/10.1016/j.apcatb.2011.07.025>

- Hua Y, Wang S, Xiao J, Cui C, Wang C (2017) Preparation and characterization of Fe<sub>3</sub>O<sub>4</sub>/gallic acid/graphene oxide magnetic nanocomposites as highly efficient Fenton catalysts. *RSC Adv* 7:28979–28986
- Huang D, Yan Q, Xue X, Ren Y, Shen Y (2020) Preparation of iron tailings-based porous substrate and its application in synthesis of Co<sub>3</sub>O<sub>4</sub> nanowires. *Conserv Util Miner Resour* 40:64–68
- Khachatryan L, Dellinger B (2011) Environmentally persistent free radicals (EPFRs)-2. Are free hydroxyl radicals generated in aqueous solutions? *Environ Sci Technol* 45:9232–9239. <https://doi.org/10.1021/es201702q>
- Kossoff D, Dubbin WE, Alfredsson M, Edwards SJ, Macklin MG, Hudson-Edwards KA (2014) Mine tailings dams: characteristics, failure, environmental impacts, and remediation. *Appl Geochem* 51:229–245. <https://doi.org/10.1016/j.apgeochem.2014.09.010>
- Kwan WP, Voelker BM (2002) Decomposition of hydrogen peroxide and organic compounds in the presence of dissolved iron and ferrihydrite. *Environ Sci Technol* 36:1467–1476. <https://doi.org/10.1021/es011109p>
- Li K, Zhao Y, Song C, Guo X (2017a) Magnetic ordered mesoporous Fe<sub>3</sub>O<sub>4</sub>/CeO<sub>2</sub> composites with synergy of adsorption and Fenton catalysis. *Appl Surf Sci* 425:526–534
- Li S, Gao L, Wen H, Li G, Wang Y (2017b) Modification and application of coking coal by alkali pretreatment in wastewater adsorption. *Sep Sci Technol* 52:2532–2539. <https://doi.org/10.1080/01496395.2017.1355383>
- Li W, Wu X, Li S, Tang W, Chen Y (2018) Magnetic porous Fe<sub>3</sub>O<sub>4</sub>/carbon octahedra derived from iron-based metal-organic framework as heterogeneous Fenton-like catalyst. *Appl Surf Sci* 436:252–262. <https://doi.org/10.1016/j.apsusc.2017.11.151>
- Li D, Yang T, Li Y, Liu Z, Jiao W (2020) Facile and green synthesis of highly dispersed tar-based heterogeneous Fenton catalytic nanoparticles for the degradation of methylene blue. *J Clean Prod* 246:1–11
- Liu W, Qian J, Wang K, Xu H, Jiang D, Liu Q, Yang X, Li H (2013) Magnetically separable Fe<sub>3</sub>O<sub>4</sub> nanoparticles-decorated reduced graphene oxide nanocomposite for catalytic wet hydrogen peroxide oxidation. *J Inorg Organomet Polym Mater* 23:907–916. <https://doi.org/10.1007/s10904-013-9863-4>
- Luo W, Zhu L, Wang N, Tang H, Cao M, She Y (2010) Efficient removal of organic pollutants with magnetic nanoscaled BiFeO<sub>3</sub> as a reusable heterogeneous Fenton-like catalyst. *Environ Sci Technol* 44:1786–1791. <https://doi.org/10.1021/es903390g>
- Neamtu M, Zaharia C, Catrinescu C, Yediler A, Macoveanu M, Kettrup A (2004) Fe-exchanged Y zeolite as catalyst for wet peroxide oxidation of reactive azo dye Procion Marine H-EXL. *Appl Catal B Environ* 48:287–294. <https://doi.org/10.1016/j.apcatb.2003.11.005>
- Pang Y, Xu Y, Chen Y, Shen S, Yin W, Wang X (2019) Experimental study on catalytic pyrolysis of pine sawdust added with Fe<sub>2</sub>O<sub>3</sub>. *J Therm Sci Technol* 18:185–190
- Park HS, Koduru JR, Choo KH, Lee B (2015) Activated carbons impregnated with iron oxide nanoparticles for enhanced removal of bisphenol A and natural organic matter. *J Hazard Mater* 286:315–324. <https://doi.org/10.1016/j.jhazmat.2014.11.012>
- Ren B, Miao J, Xu Y, Zhai Z, Dong X, Wang S, Zhang L, Liu Z (2019) A grape-like N-doped carbon/CuO-Fe<sub>2</sub>O<sub>3</sub> nanocomposite as a highly active heterogeneous Fenton-like catalyst in methylene blue degradation. *J Clean Prod* 240:1–10
- Rico M, Benito G, Salgueiro AR, Díez-Herrero A, Pereira HG (2008) Reported tailings dam failures. A review of the European incidents in the worldwide context. *J Hazard Mater* 152:846–852. <https://doi.org/10.1016/j.jhazmat.2007.07.050>
- Saleh TA, Naeemullah, Tuzen M, Sarı A (2017) Polyethylenimine modified activated carbon as novel magnetic adsorbent for the removal of uranium from aqueous solution. *Chem Eng Res Des* 117:218–227. <https://doi.org/10.1016/j.cherd.2016.10.030>
- Sharma A, Pareek V, Zhang D (2015) Biomass pyrolysis – a review of modelling, process parameters and catalytic studies. *Renew Sust Energ Rev* 50:1081–1096. <https://doi.org/10.1016/j.rser.2015.04.193>
- Silva AC, Cepera RM, Pereira MC, Lima DQ, Fabris JD, Oliveira LCA (2011) Heterogeneous catalyst based on peroxo-niobium complexes immobilized over iron oxide for organic oxidation in water. *Appl Catal B Environ* 107:237–244. <https://doi.org/10.1016/j.apcatb.2011.07.017>
- Wang D, Xiao R, Zhang H, He G (2010) Comparison of catalytic pyrolysis of biomass with MCM-41 and CaO catalysts by using TGA-FTIR analysis. *J Anal Appl Pyrolysis* 89:171–177. <https://doi.org/10.1016/j.jaap.2010.07.008>
- Wang Q, Tian S, Ning P (2014) Degradation mechanism of methylene blue in a heterogeneous Fenton-like reaction catalyzed by Ferrrocene. *Ind Eng Chem Res* 53:643–649
- Wang X, Zhao H, Li Y, Song Q, Shu X (2018) Study on releasing characteristics of pyrolysis gas products and kinetic analysis of lignite pyrolysis at different heating rates based on TG-MS. *Coal Eng* 50:140–144
- Williams P, Besler S (1996) The influence of temperature and heating rate on the slow pyrolysis of biomass. *Renew Energy* 7:233–250
- Xun T, Jianan Z, Xuekai J, Bao W (2019) Catalysis of Fe<sub>2</sub>O<sub>3</sub> for coal char pyrolysis. *J Wuhan Univ Sci Technol Univ Sci Technol* 42:117–120
- Yang XJ, Xu XM, Xu J, Han YF (2013) Iron oxychloride (FeOCl): an efficient Fenton-like catalyst for producing hydroxyl radicals in degradation of organic contaminants. *J Am Chem Soc* 135:16058–16061. <https://doi.org/10.1021/ja409130c>
- Yang J, Pan B, Li H, Liao S, Zhang D, Wu M, Xing B (2016) Degradation of p-Nitrophenol on biochars: role of persistent free radicals. *Environ Sci Technol* 50:694–700. <https://doi.org/10.1021/acs.est.5b04042>
- Yi L, Mi H, Wu Q, Xia J, Zhang B (2020) Present situation of comprehensive utilization of tailings resources in China. *Conserv Util Miner Resour* 3:814–815. <https://doi.org/10.1038/163814b0>
- Yuan SJ, Dai XH (2014) Facile synthesis of sewage sludge-derived mesoporous material as an efficient and stable heterogeneous catalyst for photo-Fenton reaction. *Appl Catal B Environ* 154:252–258. <https://doi.org/10.1016/j.apcatb.2014.02.031>
- Zhang H, Xue G, Chen H, Li X (2018) Magnetic biochar catalyst derived from biological sludge and ferric sludge using hydrothermal carbonization: preparation, characterization and its circulation in Fenton process for dyeing wastewater treatment. *Chemosphere* 191:64–71. <https://doi.org/10.1016/j.chemosphere.2017.10.026>
- Zheng J, Gao Z, He H, Yang S, Sun C (2016) Efficient degradation of acid orange 7 in aqueous solution by iron ore tailing Fenton-like process. *Chemosphere* 150:40–48. <https://doi.org/10.1016/j.chemosphere.2016.02.001>
- Zhu S, Huang X, Ma F, Wang L, Duan X, Wang S (2018) Catalytic removal of aqueous contaminants on N-doped graphitic biochars: inherent roles of adsorption and nonradical mechanisms. *Environ Sci Technol* 52:8649–8658. <https://doi.org/10.1021/acs.est.8b01817>

**Publisher's note** Springer Nature remains neutral with regard to jurisdictional claims in published maps and institutional affiliations.